

## Manipulation of Förster Energy Transfer of Coupled Fluorophores Through Biotransformation by *Pseudomonas resinovorans* CA10

Michael A. Daniele, Yuriy P. Bandera and Stephen H. Foulger\*

Center for Optical Materials Science and Engineering Technologies, School of Materials Science and Engineering, Clemson University, Clemson, SC

Received 25 July 2011, accepted 22 October 2011, DOI: 10.1111/j.1751-1097.2011.01023.x

### ABSTRACT

An alkyne-terminated anthracene and azide-terminated carbazole were joined through a copper-catalyzed cycloaddition to form a joined donor/acceptor pair. The photonic pair exhibited energy transfer when excited at the peak absorbance of carbazole and fluoresced with an anthracene spectral response. The fluorescent behavior was confirmed as Förster energy transfer (FRET). The lysate of *Pseudomonas resinovorans* CA10, a member of a predominant group of soil microorganisms that can metabolize a host of substrates, was employed to degrade the pair and alter the luminance spectral characteristics. The FRET was diminished and the corresponding, individual fluorescence of carbazole and anthracene returned. This general approach may find applications in single-cell metabolic studies and bioactivity assays.

### INTRODUCTION

The most widely utilized technique for the detection and targeting of endogenous proteins through fluorescence relies on the labeling of the protein with a primary antibody and subsequent attachment of a complementary, emitting dye, protein or particle (1). For decades, employing a chromophore pair that can participate in Förster resonance energy transfer (FRET) has been the operational basis for studying protein dynamics. For example, protein conformational changes, protein–protein interactions and protein synthesis are measurable as a result of dependence of the FRET efficiency on the separation distance and orientation of the donor and acceptor (2). Recently, techniques employing FRET have been employed in metabolomics, which focuses on the collection of metabolites (metabolome) in a biologic cell, tissue, organ or organism, which are the end products of cellular processes (3). Establishing the processes that generate the metabolome provides insights into the biochemical diversity of cell populations. To achieve this level of understanding requires a method for single-cell metabolomic studies (4).

Xenobiotic metabolism, as expressed by *Pseudomonas* spp., is a model of the complicated metabolite network present in many soil microorganisms that will require new sensory and

analytic technologies to unlock critical steps in metabolic pathways (5). *Pseudomonas* spp. is the most predominant group of soil microorganisms that degrade carbazole, a heterocyclic aromatic contaminant produced by oil refinement. *Pseudomonas resinovorans* CA10, found and cultivated from contaminated soil sites (6), has been exploited for bioremediation, environmental and biotechnology research (7–12); therefore, rapid detection of carbazole-degrading activity and understanding of this process can improve efficacy of bioremediation and industrial efforts.

Differing species of carbazole degraders all appear to follow a similar carbazole degradation pathway that begins with the oxidative cleavage of the heterocyclic nitrogen ring of carbazole, catalyzed by carbazole 1,9a-dioxygenase (CARDO); subsequent breakdown of carbazole requires the degradation of one of the aromatic rings, meaning *P. resinovorans* CA10 also produces a meta-cleavage enzyme, 2-aminobiphenyl-2,3-diol-1,2-dioxygenase (13). Previous studies indicate that CARDO can catalyze diverse oxygenation reactions and has a broad substrate range, including polycyclic aromatic hydrocarbons, such as dibenzothiophene, biphenyl and polycyclic aromatic hydrocarbons and is attributed to flexibility in binding of substrates to the active site of CARDO (14). This flexibility allows for the introduction of marker compounds tethered to native substrates. To this end, a donor/acceptor pair was covalently linked and their FRET characteristics employed in the detection of a metabolic transformation, when exposed to the CARDO containing *P. resinovorans* CA10 lysate.

### MATERIALS AND METHODS

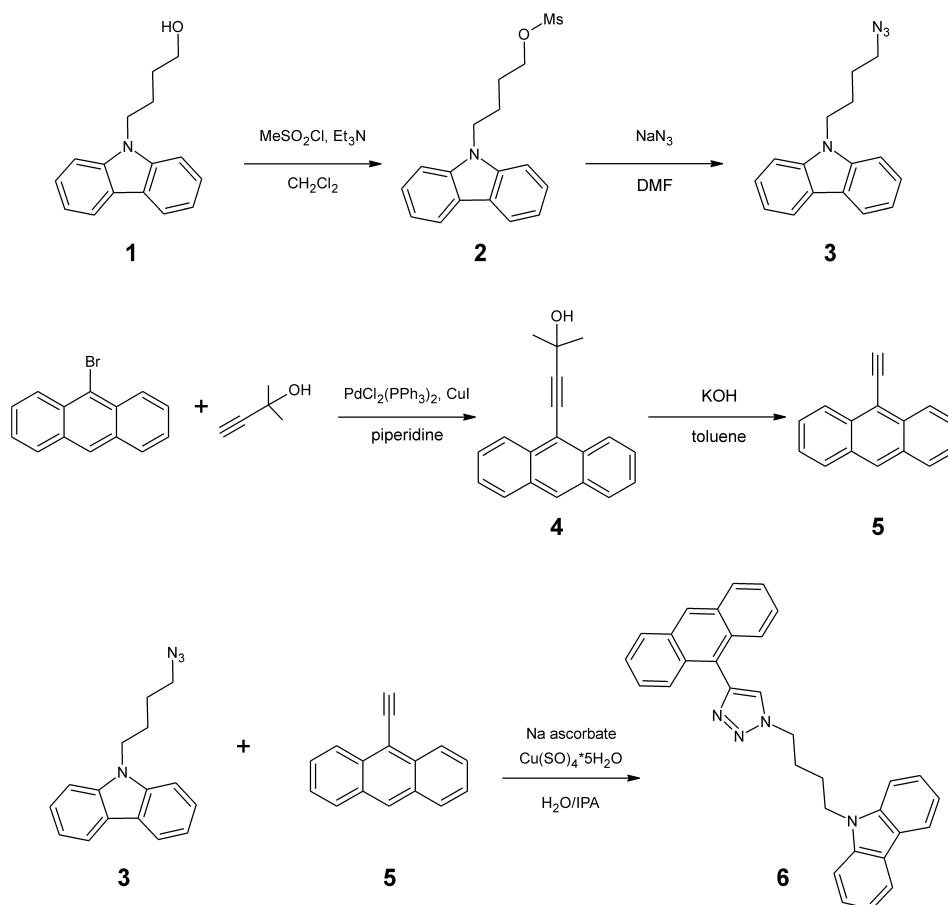
**Reagents and solvents.** All the commercial reagents were used without further purification. All the solvents were dried according to standard methods. Deionized water was obtained from a Nanopure System and exhibited a resistivity of approximately  $10^{18} \text{ ohm}^{-1} \text{ cm}^{-1}$ .

**Characterization.**  $^1\text{H}$  and  $^{13}\text{C}$  NMR spectra were recorded on JEOL ECX-300 spectrometers (300 and 76 MHz for proton and carbon, respectively). Chemical shifts for protons are reported in parts per million downfield from tetramethylsilane and are referenced to residual protium in the NMR solvent ( $\text{CDCl}_3$ :  $\delta$  7.26 ppm,  $\text{DMSO-}d_6$ :  $\delta$  2.50 ppm). Chemical shifts for carbons are reported in parts per million downfield from tetramethylsilane and are referenced to the carbon resonances of the solvent ( $\text{CDCl}_3$ :  $\delta$  77.16,  $\text{DMSO-}d_6$ :  $\delta$  39.52 ppm). Electron impact (EI) (70 eV) ionization mass spectra were obtained using Shimadzu GC-17A mass spectrometer. LC/MS mass spectra were obtained using Finnigan LCQ spectrometer and HP 1100 (HPLC). Photoluminescence (PL) and photoluminescence excitation

\*Corresponding author email: foulger@clemson.edu (Stephen Foulger)

© 2011 Wiley Periodicals, Inc.

Photochemistry and Photobiology © 2011 The American Society of Photobiology 0031-8655/12



**Scheme 1.** Reaction scheme for synthesis of ATBC and starting compounds.

(PLE) spectra were collected using a Jobin-Yvon Fluorolog 3-222 Tau spectrometer. Spectral imaging was collected using a Thermo Oriol xenon arc lamp (Thermo Oriol 66902) mated with a Thermo Oriol Cornerstone 7400 1/8 m monochromator (Thermo Oriol 7400) and a Horiba Jobin-Yvon MicroHR spectrometer coupled with a Synapse CCD detector.

**Synthesis of donor/acceptor system.** Compounds 1 and 5 were synthesized according to published methods (15,16; Scheme 1).

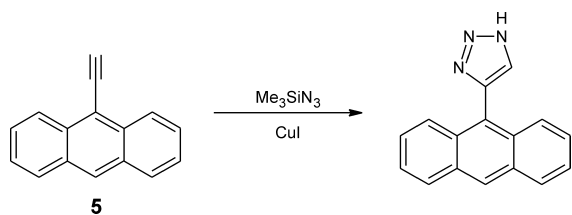
**Synthesis of 4-(9H-carbazol-9-yl)butyl methanesulfonate (2).** To a cooled solution of 4-(9H-carbazol-9-yl)butan-1-ol (1) (3.0 g, 12.5 mmol) and triethylamine (2.53 g, 25.0 mmol) in dichloromethane (30 mL), a solution of methanesulfonyl chloride (2.01 g, 17.6 mmol) in dichloromethane (2 mL) was added drop-wise. The solution was stirred for 8 h at room temperature and then washed with water. The organic layer was separated, dried with  $\text{Na}_2\text{SO}_4$  and then filtered. The solvent was removed under reduced pressure to give clear brown oil (3.3 g). Yield 83%. This product was used in the next step without further purification.  $^1\text{H}$  NMR ( $\text{CDCl}_3$ )  $\delta$  1.76 (m, 2H,  $^3J_{\text{HH}} = 6.3$  Hz), 2.00 (m, 2H,  $^3J_{\text{HH}} = 6.8$  Hz), 2.88 (s, 3H), 4.13 (t, 2H,  $^3J_{\text{HH}} = 6.3$  Hz), 4.36 (t, 2H,  $^3J_{\text{HH}} = 6.8$  Hz), 7.22–7.28 (m, 2H,  $^3J_{\text{HH}} = 7.9$  Hz), 7.37–7.51 (m, 4H), 8.12 (d, 2H,  $^3J_{\text{HH}} = 7.9$  Hz).

**Synthesis of 9-(4-azidobutyl)-9H-carbazole (3).** A mixture of 3-(9H-carbazol-9-yl)butyl methanesulfonate (2; 3.3 g, 10.4 mmol) and sodium azide (1.35 g, 20.8 mmol) in dimethylformamide (10 mL) was heated and stirred at 80°C for 7 h. After cooling, the mixture was quenched with water and extracted with dichloromethane. The organic solution was washed with water, dried with  $\text{Na}_2\text{SO}_4$ , filtered and filtrate was evaporated under vacuum to give red-brown oil. After purification by flash column chromatography (silicagel, hexane:dichloromethane 9:1,  $R_f = 0.2$ ) 1.8 g of clear oil was obtained. Yield 65%.  $^1\text{H}$  NMR ( $\text{CDCl}_3$ )  $\delta$  1.65 (m, 2H), 1.98 (m, 2H), 3.27 (t, 2H,  $^3J_{\text{HH}} = 6.9$  Hz), 4.36 (t, 2H,  $^3J_{\text{HH}} = 7.2$  Hz),

7.21–7.27 (m, 2H,  $^3J_{\text{HH}} = 7.9$  Hz), 7.38–7.51 (m, 4H), 8.10 (d, 2H,  $^3J_{\text{HH}} = 7.9$  Hz).  $^{13}\text{C}$  NMR ( $\text{CDCl}_3$ )  $\delta$  26.44, 26.86, 42.56, 51.32, 108.65, 119.08, 120.57, 123.01, 125.85 and 140.41. EI-Mass ( $m/z$ ; rel. intensity %): 265 ( $\text{M}^+ + 1$ ; 5), 264 ( $\text{M}^+$ ; 25), 193 (90), 180 (100), 167 (46), 152 (48), 139 (11).

**Synthesis of 4-(anthracen-10-yl)-2-methylbut-3-yn-2-ol (4).** 9-Bromoanthracene (2 g, 7.8 mmol), 2-methyl-but-3-yn-2-ol (1.3 g, 15.6 mmol),  $\text{Pd}(\text{PPh}_3)_2\text{Cl}_2$  (55 mg, 0.078 mmol),  $\text{PPh}_3$  (20 mg, 0.076 mmol) and  $\text{CuI}$  (15 mg, 0.079 mmol) were dissolved in piperidine (20 mL). This mixture was refluxed for 24 h under  $\text{N}_2$  atmosphere, and then cooled to room temperature. The residue was extracted with dichloromethane and washed with water. Organic layer was separated and dried with  $\text{Na}_2\text{SO}_4$ , filtered and evaporated. The crude product was purified using flash column chromatography (silicagel, hexane: dichloromethane 1:2,  $R_f = 0.4$ ) to give 1.32 g of yellow solid, m.p. 116–117°C. Yield 65%.  $^1\text{H}$  NMR ( $\text{CDCl}_3$ )  $\delta$  1.85 (s, 6H), 2.26 (s, 1H), 7.47–7.60 (m, 4H,  $^3J_{\text{HH}} = 8.5$  Hz,  $^3J_{\text{HH}} = 6.6$  Hz  $^4J_{\text{HH}} = 1.4$  Hz,  $^4J_{\text{HH}} = 1.7$  Hz), 8.00 (m, 2H,  $^3J_{\text{HH}} = 8.5$  Hz), 8.42 (s, 1H), 8.50 (d, 2H,  $^3J_{\text{HH}} = 8.5$  Hz).

**Synthesis of 9-4-[4-(9-anthryl)-1H-1,2,3-triazol-1-yl]butyl-9H-carbazole (6).** 9-(4-azidobutyl)-9H-carbazole (ABC; 157 mg, 0.59 mmol) and 9-ethynyl-anthracene (120 mg, 0.59 mmol) were dissolved in a mixture of isopropanol (5 mL) and water (3 mL). A water solution (0.5 mL) of  $\text{CuSO}_4 \cdot 5\text{H}_2\text{O}$  (8 mg, 0.03 mmol) was added to this solution under  $\text{N}_2$  atmosphere. After 5 min of stirring at room temperature sodium L-ascorbate (20 mg, 0.1 mmol) in water (0.5 mL) was added to the reaction. Obtained mixture was stirred at 50°C for 17 h. After cooling to room temperature, the mixture was extracted with dichloromethane and washed with water. Organic layer was separated and dried with  $\text{Na}_2\text{SO}_4$ , then filtered and evaporated. The residue was crystallized with diethyl ether, filtered and dried to give 147 mg of white solid, m.p. 182–183°C. Yield 53%.  $^1\text{H}$  NMR ( $\text{DMSO}-d_6$ )  $\delta$  1.85 (m, 2H), 2.08 (m, 2H), 4.52 (t, 2H,  $^3J_{\text{HH}} = 7.0$  Hz), 4.62



**Scheme 2.** Reaction scheme for synthesis of proposed metabolite residue 4-(9-anthryl)-1H-1,2,3-triazole.

(t, 2H,  $^3J_{\text{HH}} = 6.8$  Hz), 7.18–7.23 (m, 2H,  $^3J_{\text{HH}} = 7.2$  Hz), 7.36–7.47 (m, 4H,  $^3J_{\text{HH}} = 7.2$  Hz,  $^3J_{\text{HH}} = 8.3$  Hz), 7.51–7.56 (m, 2H,  $^3J_{\text{HH}} = 7.2$  Hz), 7.63–7.68 (m, 4H,  $^3J_{\text{HH}} = 7.2$  Hz,  $^3J_{\text{HH}} = 8.3$  Hz), 8.14–8.17 (m, 4H,  $^3J_{\text{HH}} = 7.2$  Hz,  $^3J_{\text{HH}} = 8.3$  Hz), 8.45 (s, 1H), 8.73 (s, 1H).  $^{13}\text{C}$  NMR ( $\text{CDCl}_3$ )  $\delta$  26.1, 28.2, 42.4, 50.1, 108.6, 119.2, 120.6, 123.0, 124.5, 124.7, 125.3, 125.9, 126.0, 126.2, 128.4, 128.6, 131.3, 131.4, 140.6 EI-Mass (LC/MS) ( $m/z$ ; rel. intensity): 267.27 ( $M^+ + 1$ ; 100), 222.27 (80), 180.20 (28).

**Synthesis of 4-(9-anthryl)-1H-1,2,3-triazole.** The synthesis of 1H-1,2,3-triazole. 4-(9-anthryl)-1H-1,2,3-triazole was obtained from 9-ethynylantracene and TMSN<sub>3</sub> according to the literature (17). The crude product was purified using flash column chromatography (silica gel, dichloromethane and MeOH,  $R_f = 0.1$ ). Impurities were eluted with dichloromethane, and then the remaining product was eluted with MeOH. m.p. 243–244°C. Yield 59%.  $^1\text{H}$  NMR ( $\text{DMSO}-d_6$ )  $\delta$  7.47–7.58 (m, 5H,  $^3J_{\text{HH}} = 8.3$  Hz), 7.66 (m, 2H), 8.17 (d, 2H,  $^3J_{\text{HH}} = 8.3$  Hz), 8.76 (s, 1H).  $^{13}\text{C}$  NMR ( $\text{DMSO}-d_6$ )  $\delta$  125.5, 126.4, 128.5, 130.6, 130.8 EI-Mass (ESI) ( $m/z$ ; rel. intensity %): 246.27 ( $M^+ + 1$ ; 100), 215.33 (9; Scheme 2).

**Preparation of *P. resinovorans* CA10 Lysate.** *P. resinovorans* CA10 was grown in minimal media M9 minus glucose at 30°C for 48 h. The cells were harvested using a Beckman JLA 16.250 at 10 000  $\times g$  at 4°C. The cell pellet (20 g) was resuspended in five volumes of the lysis buffer (20 mM K<sub>2</sub>HPO<sub>4</sub> [pH 7.4], 0.5 mM DTT, 10% sucrose, 0.250 M KCl, protease inhibitors: pepstatin, leupeptin, chymostatin and aprotinin 5  $\mu\text{g mL}^{-1}$  final concentration, 1 mM PMSF and 1 mM EDTA) and incubated with 1 mg mL<sup>-1</sup> lysozyme at 4°C. The resuspended cells were sonicated and subjected to ultracentrifugation using a T-1270 Sorvall rotor for 45 min at 100 000  $\times g$ . The clarified supernatant was frozen in aliquots using liquid nitrogen and stored at -80°C. The total protein concentration (5.6  $\mu\text{g mL}^{-1}$ ) was measured using Bradford's assay (18).

**Degradation of ATBC with *P. resinovorans* CA10 lysate and separation of product residues.** ATBC (0.75  $\mu\text{mol}$ ) in DMSO and NADH (100  $\mu\text{mol}$ ) were used in the sonicated lysate (500  $\mu\text{L}$ ) with 50 mM Tris-HCl buffer (ca pH 7.5). DMSO was added to aid the dispersion of ATBC in water. NADH was added in excess to ensure CARDO activity was the limiting factor in the biotransformation of ATBC. PL measurements were taken after 1 h of incubation at 30°C. After exposure to lysate for 72 h, samples were centrifuged using the Sorvall Legend Micro21 at 10 000  $g$  for 30 min. Pellet was removed and decanted. The supernatant was extracted with ethyl acetate. The ethyl acetate layer was dried with sodium sulfate. Ethyl acetate was evaporated under reduced pressure, and the remaining residue was dissolved in a 90:10 water:DMSO solution for further analysis. PL measurements were taken of the resultant supernatants at  $\lambda_{\text{ex}} = 295$  and  $\lambda_{\text{ex}} = 360$  nm.

## RESULTS AND DISCUSSIONS

### Design of FRET-based molecular probe to monitor dioxygenating activity

The focus of this study was to modulate the Förster energy transfer of coupled fluorophores through their biotransformation compared with Fig. 1. Specifically, an alkyne-functionalized anthracene and azide-functionalized carbazole derivative were employed as the donor/acceptor pair and linked through a copper-catalyzed azide/alkyne cycloaddition ("click"

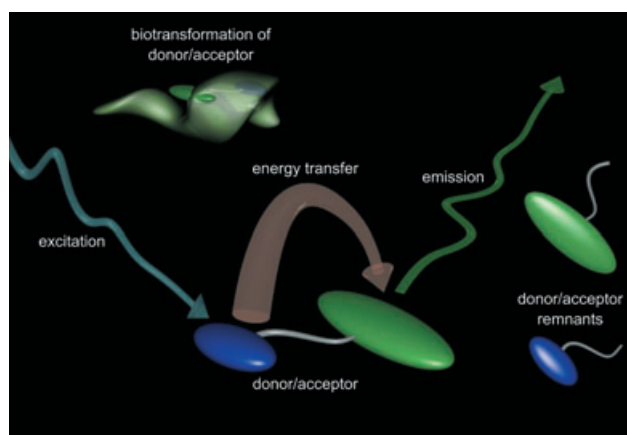


**Figure 1.** Schematic of the biotransformation of 9-4-[4-(9-anthryl)-1H-1,2,3-triazol-1-yl]butyl-9H-carbazole (ATBC), a coupled donor-acceptor pair, with exposure to the lysate of *P. resinovorans* CA10. FRET between moieties of ATBC is interrupted by enzymatic breakdown of ATBC by carbazole 1,9a-dioxygenase.

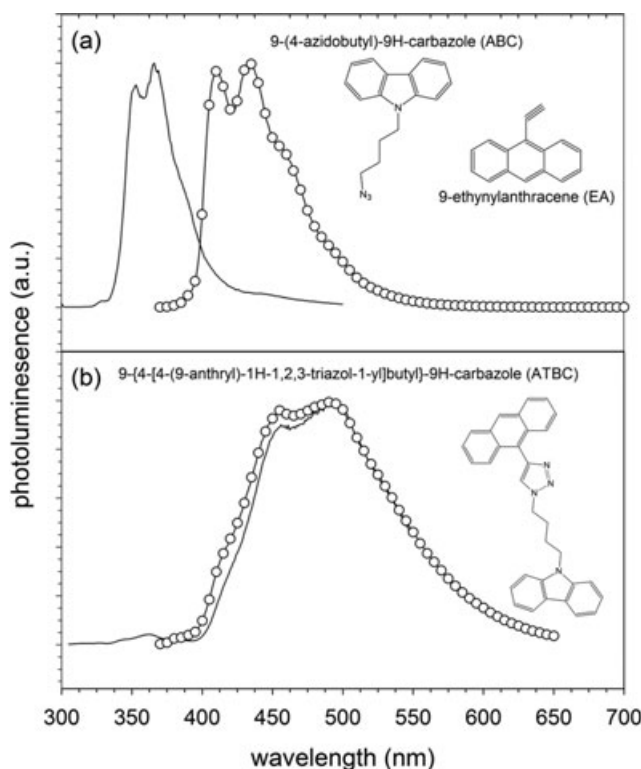


**Figure 2.** Photoluminescence of (a) 9-(4-azidobutyl)-9H-carbazole (ABC) (—) ( $\lambda_{\text{ex}} = 295$  nm) and 9-ethynylantracene (EA) (○) ( $\lambda_{\text{ex}} = 360$  nm); (b) 9-4-[4-(9-anthryl)-1H-1,2,3-triazol-1-yl]butyl-9H-carbazole (ATBC) with  $\lambda_{\text{ex}} = 295$  nm (—) and  $\lambda_{\text{ex}} = 360$  nm (○). Upon linkage of ABC and EA to form ATBC, energy is transferred through FRET and only the emission of EA is produced. All samples in 90:10 water:DMSO solution.

transformation) performed in water: isopropanol (5:4) mixture (19). CARDO catalyzes the angular dioxygenation of carbazole to yield an unstable dihydroxylated intermediate, which is considered instantly converted to 2'-aminobiphenyl-2,3-diol, whereas CARDO transforms anthracene into *cis*-1,2-dihydroxy-1,2-dihydroanthracene<sub>5</sub>. Figure 2 presents the

photoluminescence (PL) spectra and structures employed in this effort. Specifically, Fig. 2a presents the emission characteristics of both ABC and 9-ethynylantracene (EA) in water:DMSO (90:10) mixture. The carbazole-containing moiety (ABC) exhibits an emission that is characteristic of 9H-carbazole containing compounds with two major peaks at 351 and 363 nm and a shoulder at approximately 380 nm (20). Similarly, the anthracene containing moiety (EA) indicates vibronic bands in the region 410–500 nm typically seen with this chromophore when excited at 360 nm (21). In contrast to these isolated chromophores, Fig. 2b presents the emission characteristics under various excitation energies of the resulting molecule when ABC and EA have undergone a click transformation to form 9-4-(4-[9-anthryl]-1H-1,2,3-triazol-1-yl)-butyl-9H-carbazole (ATBC). With an excitation energy at a wavelength of 295 nm, there is only a small emission contribution attributed to the carbazole moiety, whereas with an excitation at 360 nm, all contributions of the carbazole are absent. Nonetheless, at both excitation energies, the emission of the linked carbazole/anthracene molecule is similar and reminiscent of an aggregated anthracene (9). The lack of a significant carbazole signature in the linked moiety with an excitation of 295 nm is indicative of energy transfer from the carbazole to anthracene. For the current system, the Förster radius was calculated to be approximately 19 Å, whereas a similar system composed of 9-phenyl carbazole and 9-cyano anthracene fabricated into Langmuir-Blodgett films with interlayers of stearic acid indicated a Förster radius of 12.5 Å (22). The calculated Förster radius is comparable to approx-

imately 13 Å maximum separation distance of the linked chromophores in ATBC. A molecular dynamics simulation of ATBC was performed *in vacuo* utilizing the MM2 force field and indicated that the most probable conformations for ATBC at room temperature result in a slightly folded back configuration that puts the anthracene and carbazole ring centers within a separation distance 5–8 Å, indicating that energy transfer from carbazole to anthracene should dominate at this temperature. A serial dilution of ATBC was also performed, which indicated the concentrations of ATBC used in this study were sufficiently dilute that the observed PL spectra was as a result of individual chromophores, *i.e.* PL at  $\lambda_{\text{ex}} = 295$  nm and  $\lambda_{\text{ex}} = 360$  nm. The normalized serial dilution spectra are provided in Figs. S1 and S2 (Supporting Information).

### Biotransformation of ATBC with *P. resinovorans* CA10 lysate

Figure 3 presents the PL spectral image at differing excitation energies of the initial compounds and the variation in emission of ATBC with exposure to the *P. resinovorans* CA10 lysate. As previously indicated (cf. Fig. 2), ABC and EA emit at differing excitation wavelengths, approximately 295 and 360 nm, respectively (cf. Fig. 3a,b,e,f). Initially, the PL spectrum of ATBC exhibits no signature from the carbazole moiety by the absence of any appreciable emission between 340 and 400 nm with either excitation energy in Fig. 3c,g, but with the introduction of the lysate, the characteristic PL signature of the carbazole moiety re-emerges as a high energy band in Fig. 3d. As a simple diagnostic tool, the reappearance of this

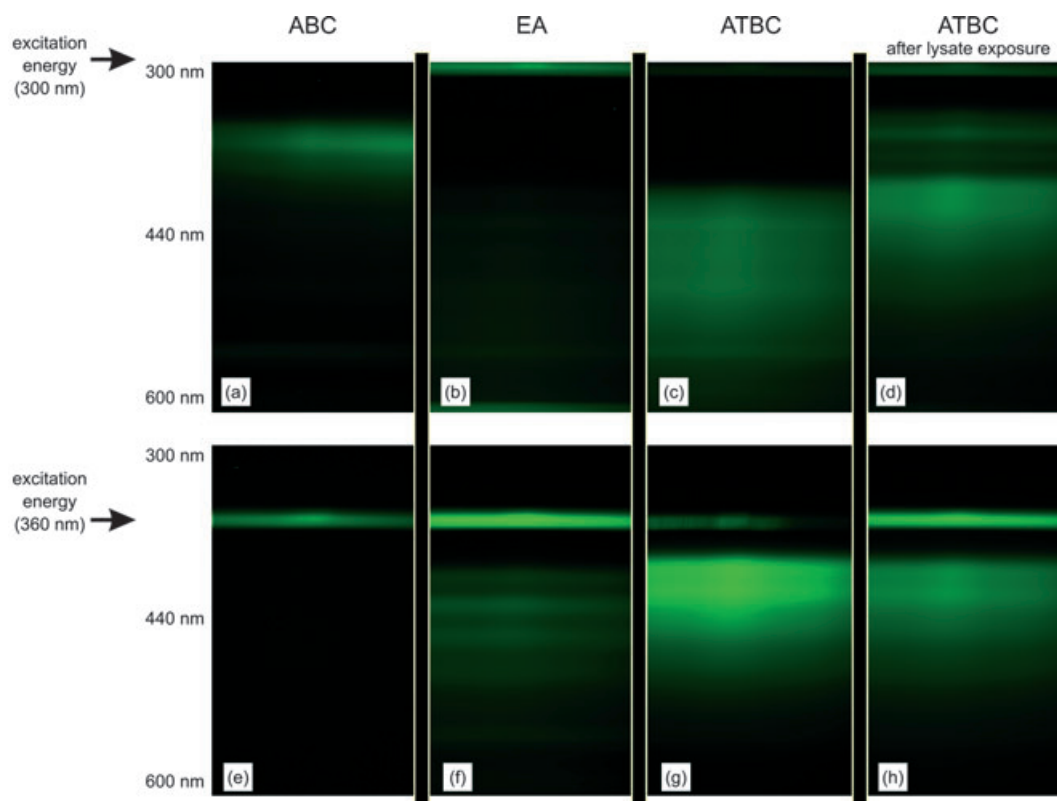


**Figure 3.** Spectral photoluminescence images of neat (a,e) ABC, (b,f) EA, (c,g) ATBC and (d,h) ATBC after exposure to the lysate of *P. resinovorans* CA10. Upper band of images (a–d) corresponds to an excitation at a wavelength of 300 nm, whereas the lower band (e–h) corresponds to 360 nm.

band in the PL image is a clear indication that some of the coupled chromophores have been separated. This was confirmed in Fig. 4a, which presents the spectral characteristics of this emission and indicates a carbazole emission coupled with a shoulder at approximately 420 nm and an enhancement of emission intensity of the peak at approximately 440 nm. These latter changes are suggestive of the re-emergence of the isolated anthracene emission being coupled to the ATBC emission, likely because of the separation of linked carbazole and anthracene moieties with the lysate degradation of the triazole linking unit.

The solution utilized in Figs. 3 and 4a includes both the reactants (proteins and ATBC) and products (residues of ABC and EA) of the enzymatic degradation and was centrifuged and redispersed multiple times in an attempt to isolate moieties. The PL spectrum of the supernatant produced in this cleaning process is presented in Fig. 4b under various excitation energies. The use of 295 and 360 nm excitation wavelengths was an attempt to isolate the contributions from the various chromophores that may be present in the solution after the enzymatic degradation of ATBC. With an excitation at 295, it is apparent that the supernatant incorporates a significant quantity of a carbazole-containing residue by the appearance of the signature 9H-carbazole PL emissions, with peaks at 351

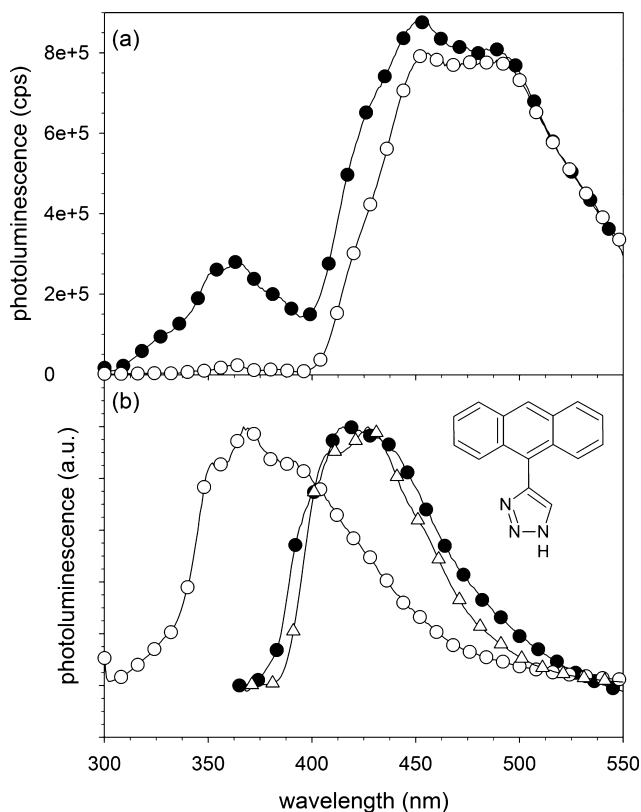


**Figure 4.** Photoluminescence of (a) ATBC ( $\lambda_{\text{ex}} = 295$  nm) initially ( $\circ$ ) and after a 1 h exposure to lysate ( $\bullet$ ) in 90:10 Tris-HCl aqueous buffer (50 mM):DMSO and of (b) supernatant (product residues) with excitation of  $\lambda_{\text{ex}} = 295$  nm ( $\circ$ ) and  $\lambda_{\text{ex}} = 360$  nm ( $\bullet$ ) and 4-(9-anthryl)-1H-1,2,3-triazole (structure in inset) with excitation of  $\lambda_{\text{ex}} = 360$  nm ( $\triangle$ ) in DMSO. Rise in spectral response between 300 and 400 nm (Fig. 4a) is representative of the degradation of ATBC by *P. resinovorans* CA10 lysate. The emission of product residues (Fig. 4b) is comparable to those of neat ABC and EA.

and 366 nm. In addition, in Fig. 4b, the carbazole PL emission has a small shoulder at 393 nm, a peak attributed to the anthracene moiety. With an excitation wavelength of 360 nm, the PL characteristics of the supernatant exhibit characteristics of ATBC as well as an aggregated anthracene. For comparison, in Fig. 4b, the PL spectra of 4-(9-anthryl)-1H-1,2,3-triazole (AT) is presented. This compound serves as a reference acceptor assuming that the carbazole moiety was cleaved from ATBC in the biotransformation. This reference acceptor and supernatant have closely matched PL characteristics when excited at 360 nm. The separated reaction products were also subjected to mass spectroscopy analysis. ATBC incubated with *P. resinovorans* CA10 lysate and resultant metabolites were extracted from the incubation medium and products were identified by comparing mass peaks with those of pure ATBC, ABC and EA. The former showed significant fragments at  $m/z$  167, 205 and 200. These metabolites can be tentatively identified as 9-H carbazole, EA and ATBC fragment, respectively. A comparative plot of mass spectra is provided in Fig. S3. Results verified the biotransformation of ATBC by *P. resinovorans* CA10; however, there was no overt preference indicated for the degradation of either ABC or EA moieties.

To further identify the resultant metabolites and contributing components to the PL signatures in Fig. 4, the photoluminescence excitation (PLE) at various emission wavelengths was studied and is presented in Fig. 5. Setting the emission wavelength to 360 nm resulted in an excitation profile, as expected, that is indicative of the absorbance spectrum of carbazole with two main peaks centered at approximately 332 and 343 nm. Raising the emission wavelength to 410 nm resulted in an enhanced contribution from residues containing

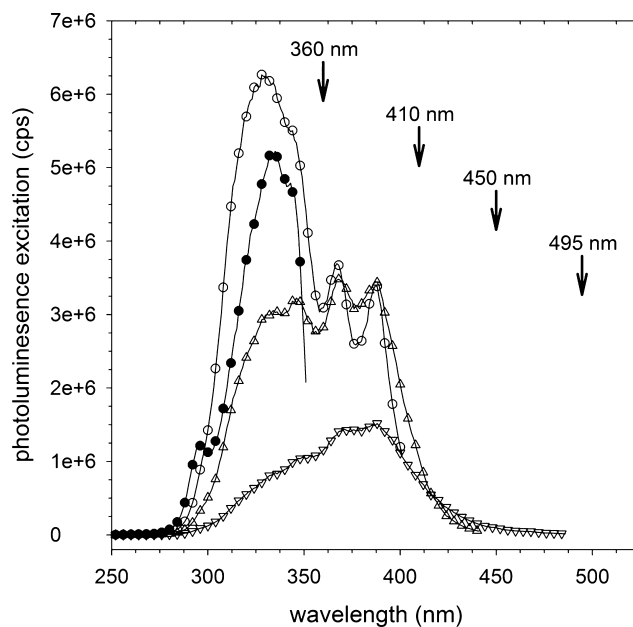


**Figure 5.** Photoluminescence excitation of supernatant (product residues) with emission at  $\lambda_{\text{em}} = 360$  nm ( $\bullet$ ),  $\lambda_{\text{em}} = 410$  nm ( $\circ$ ),  $\lambda_{\text{em}} = 450$  nm ( $\triangle$ ), and  $\lambda_{\text{em}} = 495$  nm ( $\nabla$ ). All samples in 90:10 Tris-HCl aqueous buffer (50 mM):DMSO. Varied excitation wavelengths elucidate the generating energies for product residue emission and can be correlated to the components of degraded ATBC (see text for further details).

the carbazole moiety, as well as residues that incorporate an anthracene fluorophore. The anthracene signature, as indicated by the two peaks at 381 and 403 nm, is significantly less than the contribution from carbazole-containing residues, which occurs at wavelengths under 360 nm. This indicates that the emission at 410 nm can be efficiently achieved by exciting the carbazole moiety and transferring energy to the anthracene moiety; it also suggests that the supernatant has a mixture of residues that incorporate ABC and EA, as well as ATBC. Increasing the emission wavelength to 450 nm is sufficient to remove contributions that are directly attributed to the carbazole moiety, though this wavelength is in the middle of the emission spectrum for both EA and ATBC. Nonetheless, the PLE spectrum at this emission wavelength indicates a contribution from the carbazole fluorophore, suggesting that either the supernatant contains (1) ATBC and/or (2) carbazole and anthracene fluorophores that are not chemically linked, but spatially within the Förster radius for energy transfer. Extending the emission wavelength to 495 nm verifies that the supernatant must contain ATBC as this fluorophore would be the dominating emitter at this wavelength.

## CONCLUSION

In summary, a simple diagnostic tool was presented that employed a coupled donor/acceptor pair that was formed through a click transformation. The FRET pair exhibited a significant variation in PL response with exposure to the *P. resinovorans* CA10 lysate, an organism that can degrade variants of both the donor and acceptor fluorophores. This general approach can be tailored for a range of metabolic processes and be employed as a method for single cell metabolic studies.

*Acknowledgements*—The authors thank DARPA (grant number: N66001-04-1-8933), the State of South Carolina, and the Gregg-Graniteville Foundation for financial support.

## SUPPORTING INFORMATION

Additional Supporting Information may be found in the online version of this article:

**Figure S1.** Photoluminescence spectrum for the serial dilution of ATBC normalized to the mass of chromophore at  $\lambda_{\text{ex}} = 295$  nm.

**Figure S2.** Photoluminescence spectrum for the serial dilution of ATBC normalized to the mass of chromophore at  $\lambda_{\text{ex}} = 360$  nm.

**Figure S3.** Mass spectroscopy comparison for donor-acceptor system (ATBC), paired moieties (ABC, EA) and biotransform residues of ATBC (CA10 biotransformation).

Please note: Wiley-Blackwell is not responsible for the content or functionality of any supporting information supplied by the authors. Any queries (other than missing material) should be directed to the corresponding author for the article.

## REFERENCES

- Giepmans, B. N. G., S. R. Adams, M. H. Ellisman and R. Y. Tsien (2006) The fluorescent toolbox for assessing protein location and function. *Science* **312**, 217–224.
- Förster, T. (1946) Energiewanderung und Fluoreszenz. *Naturwissenschaften* **6**, 166–175.
- Prasuhn, D. E., A. Feltz, J. B. Blanco-Canosa, K. Susumu, M. H. Stewart, B. C. Mei, A. V. Yakovlev, C. Loukov, J. M. Mallet, M. Oheim, P. E. Dawson and I. L. Medintz (2010) Quantum dot peptide biosensors for monitoring caspase-3 proteolysis and calcium ions. *ACS Nano*, **4**, 5487–5497.
- Amantonico, A., P. L. Urban and R. Zenobi (2010) Analytical techniques for single-cell metabolomics: state of the art and trends. *Anal. Bioanal. Chem.* **398**, 2493–2504.
- Patterson, A. D., F. J. Gonzalez and J. R. Idle (2010) Xenobiotic metabolism: a view through the metabolometer. *Chem. Res. Toxicol.* **23**, 851–860.
- Ouchiya, N., Y. Zhang, T. Omori and T. Kodama (1993) Biodegradation of carbazole by *Pseudomonas* spp. CA06 and CA10. *Biosci. Biotechnol. Biochem.* **57**, 455–460.
- Ahuja, S. K., G. M. Ferreira and A. R. Moreira (2004) Utilization of enzymes for environmental applications. *Crit. Rev. Biotechnol.* **24**, 125–154.
- Seo, J. S., Y. S. Keum and Q. X. Li (2009) Bacterial degradation of aromatic compounds. *Int. J. Environ. Res. Public Health*, **6**, 278–309.
- Wang, X., Z. H. Gai, B. Yu, J. H. Feng, C. Y. Xu, Y. Yuan, Z. X. Lin and P. Xu (2007) Degradation of carbazole by microbial cells immobilized in magnetic gellan-gum gel beads. *Appl. Environ. Microbiol.* **73**, 6421–6428.
- Larentis, A. L., H. C. C. Sampaio, C. C. Carneiro, O. B. Martins and T. L. M. Alves (2011) Evaluation of growth of carbazole biodegradation and anthranilic acid production. *Braz. J. Chem. Eng.* **28**, 37–44.
- Habe, H., K. Ide, M. Yotsumoto, H. Tsuji, H. Hirano, J. Widada, T. Yoshida, H. Nojiri and T. Omori (2001) Preliminary examinations for applying a carbazole-degrader, *Pseudomonas* spp. strain CA10, to dioxin-contaminated soil remediation. *Appl. Microbiol. Biotechnol.* **56**, 788–795.
- Waldau, D., K. Methling, A. Mikolasch and F. Schauer (2009) Characterization of new oxidation products of 9H-carbazole and structure related compounds by biphenyl-utilizing bacteria. *Appl. Microbiol. Biotechnol.* **81**, 1023–1031.
- Nojiri, H., H. Habe and T. Omori (2001) Bacterial degradation of aromatic compounds via angular dioxygenation. *J. Gen. Appl. Microbiol.* **47**, 279–305.
- Nojiri, H., J. W. Nam, M. Kosaka, K. I. Morii, T. Takemura, K. Furihata, H. Yamane and T. Omori (1999) Diverse oxygenations catalyzed by carbazole 1,9a-dioxygenase from *Pseudomonas* sp. strain CA10. *J. Bacteriol.* **181**, 3105–3113.
- Guan, J., D. E. Kyle, L. Gerena, Q. A. Zhang, W. K. Milhous and A. J. Lin (2002) Design, synthesis, and evaluation of new chemosensitizers in multi-drug-resistant *Plasmodium falciparum*. *J. Med. Chem.* **45**, 2741–2748.
- Xiao, Q., R. T. Ransinghe, A. M. P. Tang and T. Brown (2007) Naphthalenyl- and anthracenyl-ethynyl dT analogues as base discriminating fluorescent nucleosides and intramolecular energy transfer donors in oligonucleotide probes. *Tetrahedron* **63**, 3483–3490.
- Jin, T., S. Kamijo and Y. Yamamoto (2004) Copper-catalyzed synthesis of *N*-unsubstituted 1,2,3-triazoles from non-activated terminal alkynes. *Eur. J. Org. Chem.* **18**, 3789–3791.
- Bradford, M. M. (1976) Rapid and sensitive method for quantitation of microgram quantities of protein utilizing principle of protein-dye binding. *Anal. Biochem.* **72**, 248–254.
- Kolb, H. C., M. G. Finn and K. B. Sharpless (2001) Diverse chemical function from a few good reactions. *Angew. Chem. Int. Ed. Engl.* **40**, 2004–2021.
- Johnson, G. E. (1974) Spectroscopic study of carbazole by photoselection. *J. Phys. Chem.* **78**, 1512–1521.
- Ray, K., D. Bhattacharjee and T. N. Mishra (1997) Photophysical characteristics of 9-cyanoanthracene molecules organized in Langmuir-Blodgett films. *J. Chem. Soc. Faraday. Trans.* **93**, 4041–4045.
- Ray, K. and T. N. Mishra (1999) Energy transfer between carbazole and anthracene moieties organized in Langmuir-Blodgett films. *J. Phys. Chem. Solids* **60**, 401–405.